# CIRCULAR CYLINDRICAL DIELECTRIC ROD WAVEGUIDE

By *V. Subrahmaniam and S. K. Chatterjee

*(Department of Electrical Communication Engineering, Indian Institute of Science, Bangalore, India*

[Received : March 4, 1968]

Abstract

The propagation characteristics, such as, propagation constant, guide wavelength, radial field spread, division of power as a function of the diameter and dielectric constant of a circular cylindrical rod dielectric guide excited in $H_{01}$, $E_{01}$ and $HE_{11}$ modes are studied. The study of scattering coefficients of the $H_{01}^{\circlearrowright}$—$H_{11}^{\circlearrowleft}$ mode transducer which is used to excite the guide in $HE_{11}$ mode, leads to its representation as an equivalent Tee- network. The insertion loss and launching efficiency of the mode transducer has been evaluated. The scattering coefficients, impedance and attention characteristics of the dielectric guide excited in $HE_{11}$ mode are also studied.

## 1. Introduction

A straight infinitely long loss-free dielectric rod behaves like a waveguide in the sense that electromagnetic waves can travel along it without radiation loss. The problem of the propagation of transverse magnetic mode in a lossless dielectric guide was investigated theoretically by Hondros and Debye[1] and their theory was experimentally confirmed by Zahn[2] and by Schriever[3]. Important contributions on the theoretical aspects of dielectric rod waveguides have been made recently by Clarricoats[4] and Waldron[5, 5a]. The work by Gillespie[6] on the negtive wave impedance and power flow in a dielectric rod guide is of significant importance. Theoretical study of the propagation of backward waves in a bounded dielectric rod guide by Clarricoats and Waldron[7], Clarricoats[8] and Brown[9], has opened a new field of research. The study on the attenuation characteristics of a dielectric rod wave guide by Chandler[10] and Elasser[11] has also created an interest in the possible practical utility of a dielectric rod being used as a guide for electromagnetic waves at microwave frequencies. Several authors (Du Hamel and Duncan[12]; Angulo and Chang[13, 14]; Duncan[16]; Duncan and Du Hamel[15]), have made significant contributions on the excitation problem of a dielectric rod waveguide. The problem of radiation from the feed end of the dielectric rod guide to the discontinuity invariably present at the junction of the mode transducer and the dielectric rod has been treated by Kay[17], Brown and

* Dr. V. Subrahmaniam is an Assistant Professor at the Birla Institute of Technology and Science, Pilani, Rajasthan and was on deputation during the period of work.

Spector[18], and Weil[19]. The object of the paper is to present the results of investigations on the propagation characteristics of electromagnetic waves on unbounded circular cylindrical dielectric rod waveguide excited in $H_{01}$, $E_{01}$ and $HE_{11}$ modes at 3.2 cms. wavelength. The main emphasis is on the guide excited in $HE_{11}$ mode. It is believed that the contributions specially on the impedance characteristics, scattering coefficients, division of power of the dielectric guide, scattering coefficients of the $H_{01}^{\square} - H_{11}^{\circ}$ mode transducer and its equivalent circuit representation, the study of the insertion loss and the launching efficiency on the basis of the scattering parameters will add significantly to our existing knowledge in the field of dielectric rod waveguides

## 2. Field Components

Assuming that the circular cylindrical dielectric rod guide is infinitely extended in the direction of propagation and that there is no radiation from the rod and $\mu_1 = \mu_2 = \mu_0$, $\sigma_1 = \sigma_2 = 0$, the field components for the three modes $H_{01}$, $E_{01}$ and $HE_{11}$ inside and outside the dielectric guide (Fig. 1) are as follows

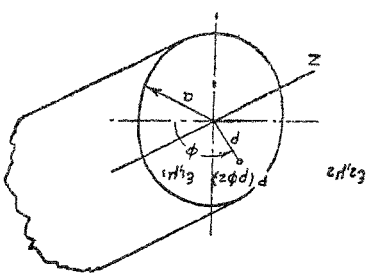


FIG. 1
The circular cylindrical coordinate system employed

*$H_{01}$ mode*:

Inside the guide. [Region 1, $(\rho \leq a)$]

$$E_{\phi 1} = -Bk_1 J_0'(k_1\rho)\exp(-\gamma_1 z)$$
$$H_{\rho 1} = B(\gamma_1 k_1/i\omega\mu_0) J_0'(k_1\rho)\exp(-\gamma_1 z)$$
$$H_{z1} = -B(k_1^2/i\omega\mu_0) J_0(k_1\rho)\exp(-\gamma_1 z) \qquad [1]$$

Outside the guide, [Region 2, $(\rho \geq a)$]

$$E_{\phi 2} = -C k_2 H_0^{(1)'}(k_2 \rho) \exp(-\gamma_2 z)$$
$$H_{\rho 2} = -C(\gamma_2 k_2 / i\omega\mu_0) H_0^{(1)'}(k_2 \rho) \exp(-\gamma_2 z)$$
$$H_{z2} = -C(k_2^2 / i\omega\mu_0) H_0^{(1)}(k_2 \rho) \exp(-\gamma_2 z) \quad [2]$$

*$E_{0i}$ mode*:

Inside the guide [Region 1, $(\rho \leq a)$]

$$E_{\rho 1} = -b(k_1 \gamma_1 / i\omega\epsilon_1) J_0'(k_1 \rho) \exp(-\gamma_1 z)$$
$$E_{z1} = b(k_1^2 / i\omega\epsilon_1) J_0(k_1 \rho) \exp(-\gamma_1 z)$$
$$H_{\phi 1} = -b k_1 J_0'(\exp(-\gamma_1 z) \quad [3]$$

Outside the guide, [Region 2, $\rho \geq a$)]

$$E_{\rho 2} = -c(k_2 \gamma_2 / i\omega\epsilon_2) H_0^{(1)'}(k_2 \rho) \exp(-\gamma_2 z)$$
$$E_{z2} = c(k_2^2 / i\omega\epsilon_2) H_0^{(1)}(k_2 \rho) \exp(-\gamma_2 z)$$
$$H_{\phi 2} = -c k_2 H_0^{(1)'}(k_2 \rho) \exp(-\gamma_2 z) \quad [4]$$

where $k^2 = \gamma^2 + \omega^2 \mu \epsilon$. The time variation is $\exp(j\omega t)$

*$HE_{11}$ mode*:

As the mode is formed by a linear combination of $H$ and $E$ modes, the following relations hold good

$$\gamma_1^E = \gamma_1^H = \gamma_1, \quad \gamma_2^E = \gamma_2^H = \gamma_2, \quad k_1^E = k_1^H = k_1, \quad k_2^E = k_2^H = k_2 \quad [5]$$

Inside the guide, [Region 1, $(\rho \leq a)$]

$$E_{\rho 1} = -B[(1/\rho) J_1(k_1 \rho) + (b/B)(\gamma_1 k_1 / i\omega\epsilon_1) J_1'(k_1 \rho)] \sin\phi \exp(-\gamma_1 z)$$
$$E_{\phi 1} = -B[k_1 J_1'(k_1 \rho) + (b/B)(1/\rho)(\gamma_1 / i\omega\epsilon_1) J_1(k_1 \rho)] \cos\phi \exp(-\gamma_1 z)$$
$$E_{z1} = B[(b/B) i k_1^2 / i\omega\epsilon_1) J_1(k_1 \rho)] \sin\phi \exp(-\gamma_1 z)$$
$$H_{\rho 1} = B[(\gamma_1 k_1 / i\omega\mu_0) J_1'(k_1 \rho) + (b/B)(1/\rho) J_1(k_1 \rho)] \cos\phi \exp(-\gamma_1 z)$$
$$H_{\phi 1} = -B[(1/\rho)(\gamma_1 / i\omega\mu_0) J_1(k_1 \rho) + (b/B) k_1 J_1'(k_1 \rho)] \sin\phi \exp(-\gamma_1 z)$$
$$H_{z1} = -B[(k_1^2 / i\omega\mu_0) J_1(k_1 \rho)] \cos\phi \exp(-\gamma_1 z) \quad [6]$$

Outside the guide, [Region 2, $(\rho \geq a)$]

$$E_{\rho 2} = -C[(1/\rho) H_1^{(1)}(k_2 \rho) + (c/C)(\gamma_2 k_2 / i\omega\epsilon_2) \times H_1^{(1)'}(k_2 \rho)] \sin\phi \exp(-\gamma_2 z)$$

$$E_{\rho 2} = -C\left[k_2 H_1^{(1)\prime}(k_2\rho) + (c/C)(1/\rho)(\gamma_2/i\omega\epsilon_2) \times H_1^{(1)}(k_2\rho)\right]\cos\phi \exp(-\gamma_2 z)$$

$$E_{z2} = -C\left[(c/C)(k_2^2/i\omega\epsilon_2) H_1^{(1)}(k_2\rho)\right]\sin\phi \exp(-\gamma_2 z)$$

$$H_{\rho 2} = C\left[(\gamma_2 k_2/i\omega\mu_0) H_1^{(1)\prime}(k_2\rho) + (c/C)(1/\rho) \times H_1^{(1)}(k_2\rho)\right]\cos\phi \exp(-\gamma_2 z)$$

$$H_{\phi 2} = -C\left[(1/\rho)(\gamma_2/i\omega\mu_0) H_1^{(1)}(k_2\rho) + (c/C) k_2 H_1^{(1)\prime}(k_2\rho)\right]\sin\phi \exp(-\gamma_2 z)$$

$$H_{z2} = -C\left[(k_2^2/i\omega\mu_0) H_1^{(1)}(k_2\rho)\right]\cos\phi \exp(-\gamma_2 z) \quad [7]$$

## 3. Characteristic Equations

By applying proper boundary conditions at the interfaces between the two media and using appropriate field components, a set of equations for the $H_{01}$, $E_{01}$ and $HE_{11}$ modes is obtained. By allowing the determinants of the coefficient $b$, $B$, $c$, and $C$ to vanish, the following determinantal equations for the respective modes are obtained.

*$H_{01}$ mode*:

$$\begin{vmatrix} k_1 J_0'(k_1 a) & -k_2 H_0^{(1)\prime}(k_2 a) \\ (k_1^2/\mu_0) J_0(k_1 a) & -(k_2^2/\mu_0) H_0^{(1)}(k_2 a) \end{vmatrix} = 0 \quad [8]$$

*$E_{01}$ mode*:

$$\begin{vmatrix} k_1 J_0'(k_1 a) & -k_2 H_0^{(1)\prime}(k_2 a) \\ (k_1^2/\epsilon_1) J_0(k_1 a) & -(k_2^2/\epsilon_2) H_0^{(1)}(k_2 a) \end{vmatrix} = 0 \quad [9]$$

*$HE_{11}$ mode*:

$$\begin{vmatrix} k_1 J_1'(k_1 a) & \frac{1}{a}\frac{\gamma}{i\omega\epsilon_1} J_1(k_1 a) & -k_2 H_1^{(1)\prime}(k_2 a) & -\frac{1}{a}\frac{\gamma}{i\omega\epsilon_2} H_1^{(1)}(k_2 a) \\ 0 & \frac{k_1^2}{i\omega\epsilon_1} J_1(k_1 a) & 0 & -\frac{k_2^2}{i\omega\epsilon_2} H_1^{(1)}(k_2 a) \\ \frac{1}{a}\frac{\gamma}{i\omega\mu_0} J_1(k_1 a) & k_1 J_1'(k_1 a) & -\frac{1}{a}\frac{\gamma}{i\omega\mu_0} H_1^{(1)}(k_2 a) & -k_2 H_1^{(1)\prime}(k_2 a) \\ \frac{k_1^2}{i\omega\mu_0} J_1(k_1 a) & 0 & -\frac{k_2^2}{i\omega\mu_0} H_1^{(1)}(k_2 a) & 0 \end{vmatrix} = 0 \quad [10]$$

The above equations lead to the following characteristic equations for the respective modes.

*$H_{01}$ mode*:

$$x_1 \frac{J_0(x_1)}{J_0'(x_1)} = x_2 \frac{H_0^{(1)}(x_2)}{H_0^{(1)\prime}(x_2)} \qquad [11]$$

*$E_{01}$ mode*:

$$x_1 \frac{J_0(x_1)}{J_0'(x_1)} = x_2 (\epsilon_1/\epsilon_2) \frac{H_0^{(1)}(x_2)}{H_0^{(1)\prime}(x_2)} \qquad [12]$$

*$HE_{11}$ mode*:

$$\left[\frac{1}{x_1}\frac{J_1'(x_1)}{J_1(x_1)} - \frac{1}{x_2}\frac{H_1^{(1)\prime}(x_2)}{H_1^{(1)}(x_2)}\right]\left[\frac{\bar{\epsilon}_1}{x_1}\frac{J_1'(x_1)}{J_1(x_1)} - \frac{1}{x_2}\frac{H_1^{(1)\prime}(x_2)}{H_1^{(1)}(x_2)}\right] = \frac{(x_1^2 - x_2^2)(x_1^2 - \bar{\epsilon}_1 x_2^2)}{x_1^4 x_2^4} \qquad [13]$$

where $x_1 = k_1 a, \quad x_2 = k_2 a$ [14]

$\bar{\epsilon}_1 = \epsilon_1/\epsilon_2$, the dielectric constant of the rod

$$x_1^2 + (x_2/i)^2 = (\pi d/\lambda_0)^2 (\bar{\epsilon}_1 - 1) \qquad [15]$$

$d = 2a$, diameter of the rod

$\lambda_0$ = Free space wavelength.

## 4. Solution of the Characteristic Equations

The characteristic equations [11, 12 and 13] have been solved for $d/\lambda_0 = 0.8$, $\bar{\epsilon}_1 = 2.6$ (see figures 2 and 3) $Y_1$ and $Y_2$ represent the left hand and right hand sides of [13] respectively. The point of intersection of the two curves gives the root $x_1$ which with [15] yields $x_2$.

## 5. Propagation Constants

The radial propagation constants $k_1$ and $k_2$ calculated from [14] are functions of $d$ and $\bar{\epsilon}_1$ of the rod (see figures 4 and 5). The axial propagation constant $\gamma$ is related to the radial propagation constant $k$ as follows:—

$$\gamma^2 = k^2 - \omega^2 \mu_0 \epsilon \qquad [16]$$

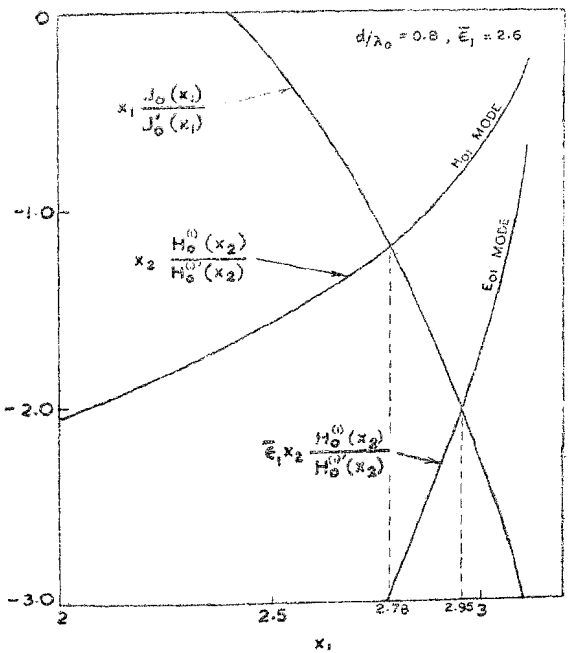


FIG. 2

Graphical solutions of the characteristic equations (1.45 & 146) for the symmetric modes

and is a function of the diameter and dielectric constant of the rod. The variations of $\gamma$ with $d/\lambda_0$ for the three modes for $\bar{\epsilon}_1 = 2.6$ and for different values of $\bar{\epsilon}_1$ in the case of $HE_{11}$ mode are represented graphically (see figures 6 and 7). As $\gamma = i\beta$ is purely imaginary, the axial phase constants represented in figures6, and 7 as ordinates are the same as the axial propagation constants in the respective cases.

## 6. Guide Wavelength

The guide wavelength, $\lambda_g$ are calculated from $x_1^2 = k_1^2 a^2$ which yields

$$\lambda_g/\lambda_0 = [\bar{\epsilon}_1 - x_1^2 (\lambda_0/\pi d)^2]^{-\frac{1}{2}} \qquad [17]$$

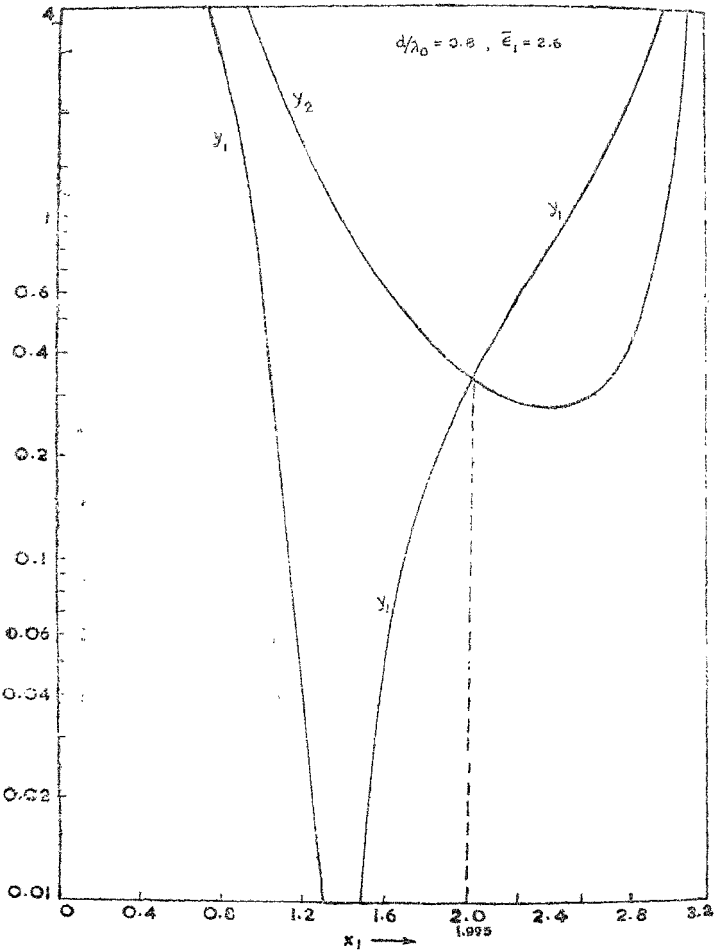


FIG. 3

Graphical solution of the characteristic equation (1.47) for the $HE_{11}$ mode

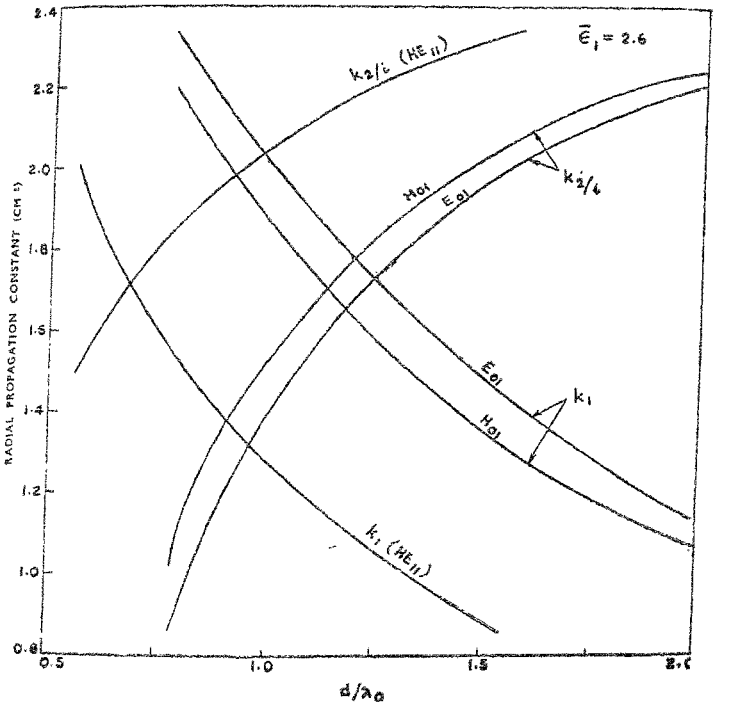


FIG. 4

Variation of radial propagation constant $k_1$ and $k_2$ with the diameter of the rod for the $H_{01}$, $E_{01}$ *and* $HB_{11}$ modes

The variations of $\lambda_g/\lambda_0$ with $d/\lambda_0$ for the three modes for $\bar{\epsilon}_1 = 2.6$ and for different values of $\epsilon_1$ in the case of $HE_{11}$ mode are represented graphically (see figures 8 and 9)

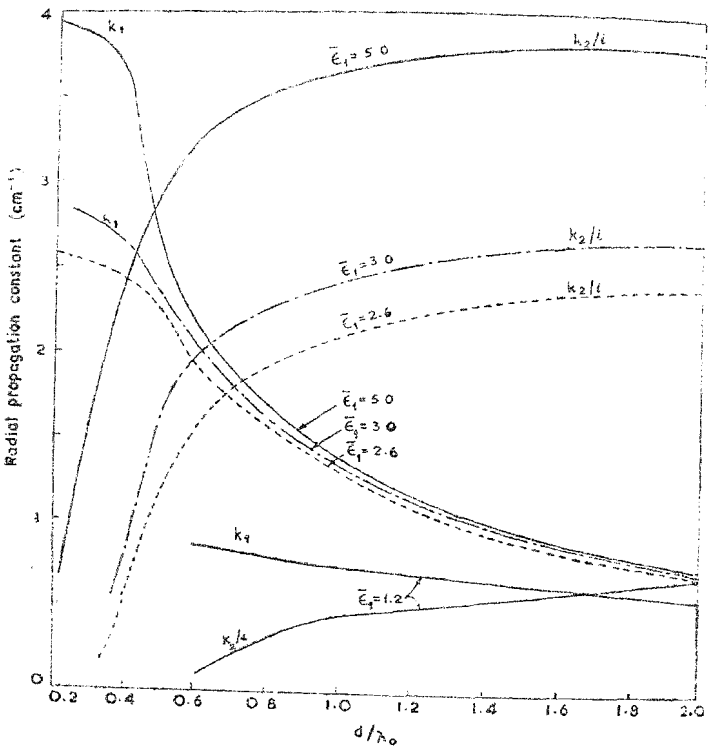


FIG. 5

Variation of radial propagation constant $k_1$ and $k_4$ with the diameter of the rod

## 7. RELATIVE POWER FLOW

The power launched in the dielectric rod will be transmitted entirely in the longitudinal direction ($z$), when there is no radiation and the dielectric rod acts entirely as a waveguide. But if some power is lost by radiation, the power will not only be transmitted in the $z$-direction but also in the radial ($\rho$)

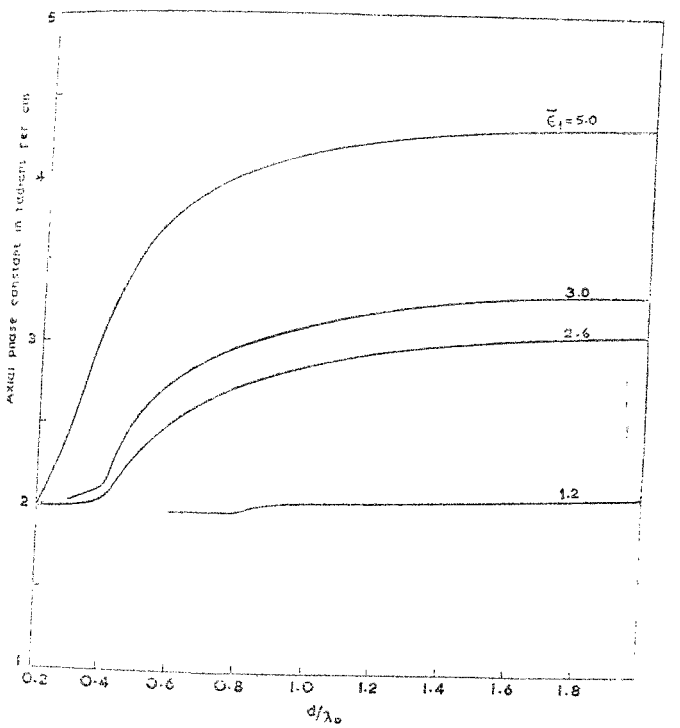


FIG. 6

Variation of the axial phase constant with the diameter of the rod

and azimuthal ($\phi$) directions. The following calculations will show the nature of power flow $P_\rho$, $P_\phi$ and $P_z$ in the $\rho$, $\phi$ and $z$ directions respectively.

$$P_\rho = \tfrac{1}{2}\, Re \iint_S \left[ E_\phi H_Z^* - E_Z H_\phi^* \right] \rho\, d\phi\, dz \qquad [18]$$

$$P_\phi = \tfrac{1}{2}\, Re \iint_S \left[ E_Z H_\rho^* - E_\rho H_Z^* \right] d\rho\, dz \qquad [19]$$

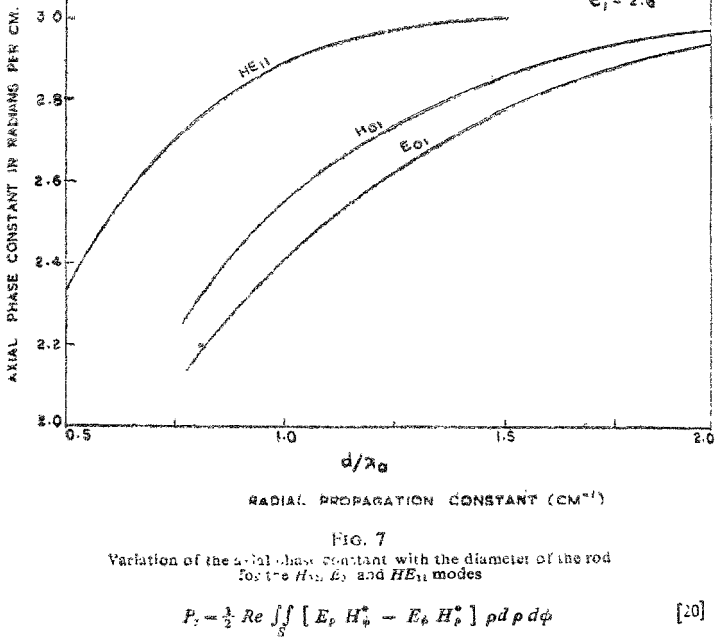


FIG. 7

Variation of the axial phase constant with the diameter of the rod for the $H_{01}$, $E_{01}$ and $HE_{11}$ modes

$$P_z = \tfrac{1}{2}\, Re \iint_S \left[ E_\rho\, H_\phi^* - E_\phi\, H_\rho^* \right] \rho d\rho\, d\phi \qquad [20]$$

where, $S$ represents the surface normal to the direction of propagation. The total power flow $P_z$ is divided mainly into two parts of which a fraction $P_z^i$ flows inside the guide ($\rho = 0$ to $\rho = a$) and the rest $P_z^0$ flows outside ($\rho = a$ to $\rho = \infty$) the guide. The limits of $\phi$ is from $\phi = 0$ to $\phi = 2\pi$. Similarly $P_\phi$ and $P_\rho$ are divided into two parts $P_\phi^i$, $P_\phi^0$ and $P_\rho^i$, $P_\rho^0$ respectively. As we are interested in the dielectric rod acting only as a guide, we may replace $\rho = a$ to $\rho = \infty$ by $\rho = a$ to $\rho = r$ in the integrals involved in the expression for $P_z^0$ and $P_\phi^0$, where $r$ represents radial distance from the axis of the rod such that the value of $P_z^0$ and $P_\phi^0$ become inappreciably small. In calculating $P_\phi^i$ and $P_\phi^0$, the limit of $z$ is from $z = 0$ to $z = l$, the length of the dielectric rod. $P_\phi^i$ and $P_\phi^0$ have been evaluated for $\phi = (\pi/4)$ as $P_\phi = 0$ for $\phi = 0$, $\pi/2$, $\pi$, $3\pi/2$ and $2\pi$. In calculating $P_\rho^i$ and $P_\rho^0$, the limit of $\phi$ is from $\phi = 0$ to $\phi = 2\pi$ and that of $z$ is from $z = 0$ to $z = l$ and $\rho = a$.

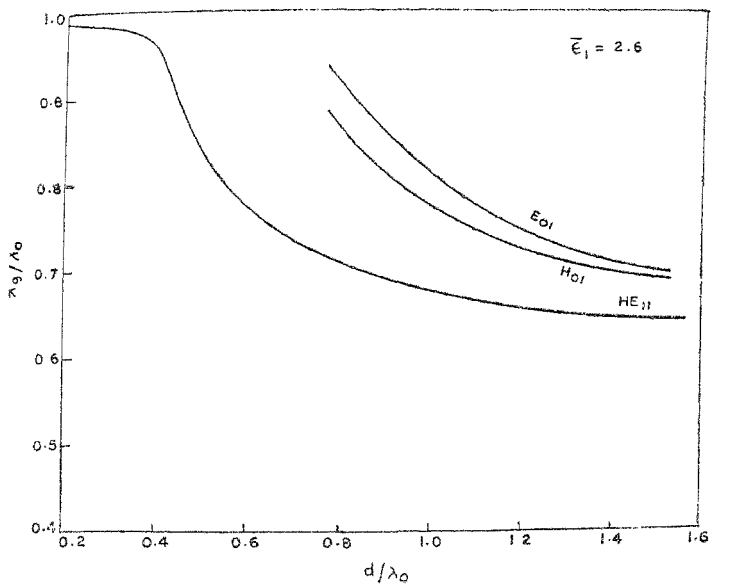


FIG. 8

Variation of the guide wavelength with the diameter of the rod for the $H_{01}$, $E_{01}$ and $H_{11}$ modes.

$$P_z^i = BB^* \left[ \frac{b}{B} \pi k_1 \left( 1 - \frac{\gamma_1^2}{\omega^2 \mu_0 \epsilon_1} \right) \int_{\rho=0}^{a} J_0 (k_1 \rho) J_1 (k_1 \rho) d\rho \right.$$

$$- \frac{\pi \gamma_1 k_1}{i\omega} \left( \frac{1}{\mu_0} + \frac{b^2}{B^2} \frac{1}{\epsilon_1} \right) \int_{\rho=0}^{a} J_0 (k_1 \rho) J_1 (k_1 \rho) d\rho$$

$$\left. + \frac{\pi \gamma_1}{i\omega} \left( \frac{1}{\mu_0} + \frac{b^2}{B^2} \frac{1}{\epsilon_1} \right) \int_{\rho=0}^{a} (1/\rho) \{ J_1 (k_1 \rho) \}^2 d\rho \right.$$

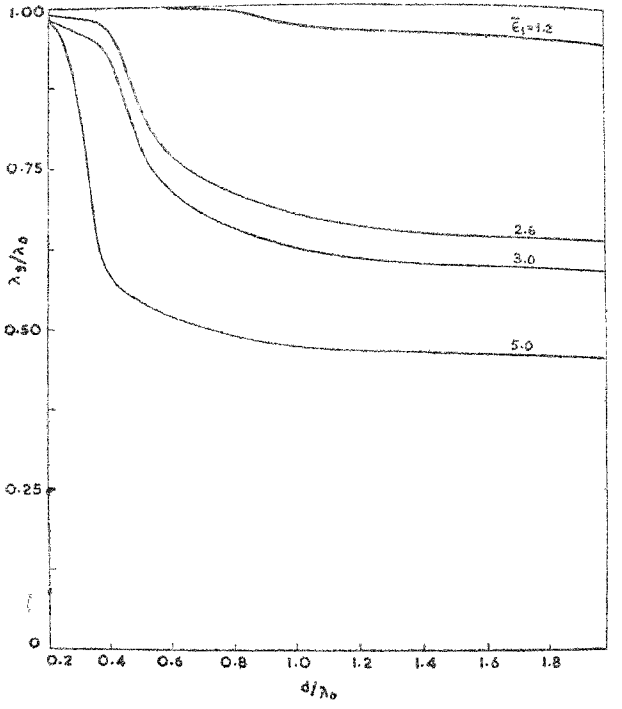


FIG. 9

Variation of the guide wavelength with the diameter of the rod for the $HE_{11}$ mode

$$- \frac{b}{B}\pi\left(1-\frac{\gamma_1^2}{\omega^2\mu_0\epsilon_1}\right)\int_{\rho=0}^{a}(1/\rho)\{J_1(k_1\rho)\}^2 d\rho$$

$$+\frac{\pi\gamma_1 k_1^2}{2j\omega}\left(\frac{1}{\mu_0}+\frac{b^2}{B^2}\frac{1}{\epsilon_1}\right)\int_{\rho=0}^{a}\rho\{J_0 k_1\rho)\}^2 d\rho\Bigg]$$

$$= BB^*[X] \qquad [21]$$

$$P_z^0 = CC^* \left[ \frac{c}{C} \pi k_2 \left( 1 - \frac{\gamma_2^2}{\omega^2 \mu_0 \epsilon_2} \right) \int_{\rho=a}^{\infty} H_0^{(1)}(k_2\rho)\, H_1^{(2)}(k_2\rho)\, d\rho \right.$$

$$- \frac{\pi \gamma_2 k_2}{i\omega} \left( \frac{1}{\mu_0} + \frac{c^2}{C^2} \frac{1}{\epsilon_2} \right) \int_{\rho=a}^{\infty} H_0^{(1)}(k_2\rho)\, H_1^{(1)}(k_2\rho)\, d\rho$$

$$+ \frac{\pi \gamma_2}{i\omega} \left( \frac{1}{\mu_0} + \frac{c^2}{C^2} \frac{1}{\epsilon_2} \right) \int_{\rho=a}^{\infty} (1/\rho) \left\{ H_1^{(1)}(k_2\rho) \right\}^2 d\rho$$

$$- \frac{c}{C} \pi \left( 1 - \frac{\gamma_2^2}{\omega^2 \mu_0 \epsilon_2} \right) \int_{\rho=a}^{\infty} (1/\rho) \left\{ H_1^{(1)}(k_2\rho) \right\}^2 d\rho$$

$$\left. + \frac{\pi \gamma_2 k_2^2}{2i\omega} \left( \frac{1}{\mu_0} + \frac{c^2}{C^2} \frac{1}{\epsilon_2} \right) \int_{\rho=a}^{\infty} \rho \left\{ H_0^{(1)}(k_2\rho) \right\}^2 d\rho \right]$$

$$= CC^* [Y] \qquad [22]$$

$$P_\phi^i = i \frac{BB^*}{4} \left[ \frac{b}{B} \frac{2l\beta_1 k_1^2}{\omega^2 \mu_0 \epsilon_1} \int_{\rho=0}^{a} (1/\rho) \left\{ J_1(k_1\rho) \right\}^2 d\rho \right.$$

$$- \frac{b}{B} \frac{2l\beta_1 k_1^3}{\omega^2 \mu_0 \epsilon_1} \int_{\rho=0}^{a} J_0(k_1\rho)\, J_1(k_1\rho)\, d\rho$$

$$\left. - \frac{lk_1^2}{\omega} \left( \frac{1}{\mu_0} + \frac{b^2}{B^2} \frac{1}{\epsilon_0} \right) \int_{\rho=0}^{a} (1/\rho) \left\{ J_1(k_1\rho) \right\}^2 d\rho \right] \qquad [23]$$

$$P_\phi^0 = i \frac{CC^*}{4} \left[ \frac{c}{C} \frac{2l\gamma_2 k_2^2}{\omega^2 \mu_0 \epsilon_2} \int_{\rho=a}^{\infty} (1/\rho) \left\{ H_1^{(1)} k_2\rho \right\}^2 d\rho \right.$$

$$- \frac{c}{C} \frac{2l\gamma_2 k_2^3}{\omega^2 \mu_0 \epsilon_2} \int_{\rho=a}^{\infty} H_0^{(1)}(k_2\rho)\, H_1^{(2)}(k_2\rho)\, d\rho$$

$$\left. - \frac{lk_2^2}{\omega} \left( \frac{1}{\mu_0} + \frac{c^2}{C^2} \frac{1}{\epsilon_2} \right) \int_{\rho=a}^{\infty} (1/\rho) \left\{ H_1^{(1)}(k_2\rho) \right\}^2 d\rho \right] \qquad [24]$$

$$P_\rho^i = i\,BB^*\left[\frac{\pi}{2}\,\frac{lk_1^3}{\omega}\,\rho\left(\frac{1}{\mu_0}-\frac{b^2}{B^2}\,\frac{1}{\epsilon_1}\right)J_0(k_1\rho)\,J_1(k_1\rho)\right.$$

$$\left.-\frac{\pi}{2}\,\frac{lk_1^2}{\omega}\left(\frac{1}{\mu_0}-\frac{b^2}{B^2}\,\frac{1}{\epsilon_1}\right)\{J_1(k_1\rho)\}^2\right] \qquad [25]$$

$$P_\rho^0 = i\,CC^*\left[\frac{\pi}{2}\,\frac{lk_2^3}{\omega}\,\rho\left(\frac{1}{\mu_0}-\frac{c^2}{C^2}\,\frac{1}{\epsilon_2}\right)H_0^{(1)}(k_2\rho)\,H_1^{(1)}(k_2\rho)\right.$$

$$\left.-\frac{\pi}{2}\,\frac{lk_2^2}{\omega}\left(\frac{1}{\mu_0}-\frac{c^2}{C^2}\,\frac{1}{\epsilon_2}\right)\{H_1^{(1)}(k_2\rho)\}^2\right] \qquad [26]$$

The values of $P^i$ and $P^0$ in the $\rho$, $\phi$, $z$ directions have been calculated as a function of $d/\lambda_0$ for perspex rod ($\bar{\epsilon}_1 = 2.6$). It is found that the power flow in the radial and circumferential direction is reactive. So in calculating the total power flow we will consider only $P_z$. The relative percentage power flowing inside the guide is

$$\frac{P_z^i}{P_z} = \frac{P_z^i/P_z^0}{(1+P_z^i/P_z^0)} \times 100 \qquad [27]$$

which is function of $d/\lambda_0$ and $\bar{\epsilon}_1$ (See figures 10 and 11)

## 8. CONSTANT PERCENTAGE POWER CONTOUR

The amount of the relative power flow outside the guide can be represented more clearly from the constant percentage power contours round the guide which are determined as follows. If $\rho = r_1, r_2, r_3 \cdots r_n$ represent the radii of the circles representing the contours inside which constant powers $P_{z1}, P_{z2}, P_{z3} \cdots P_{zn}$ flowing along the rod are located, then the ratio of the powers with respect to the total power $P_{zn}$ is

$$\begin{aligned} P_{z1} \mid P_{zn} &= W_1 \text{ at } \rho = r_1 \\ P_{z2} \mid P_{zn} &= W_2 \text{ at } \rho = r_2 \\ &\vdots \qquad\quad \vdots \\ P_{zn} \mid P_{zn} &= W_n \text{ at } \rho = r_n \end{aligned} \qquad [28]$$

where,

$$\begin{aligned} P_{z1} &= P_{z1}^i + P_{z1}^0 \text{ contained within a radius } \rho = r_1 \\ P_{z2} &= P_{z2}^i + P_{z2}^0 \text{ contained within a radius } \rho = r_2 \\ &\vdots \\ P_{zn} &= P_{zn}^i + P_{zn}^0 \text{ contained within a radius } \rho = r_n \end{aligned} \qquad [29]$$

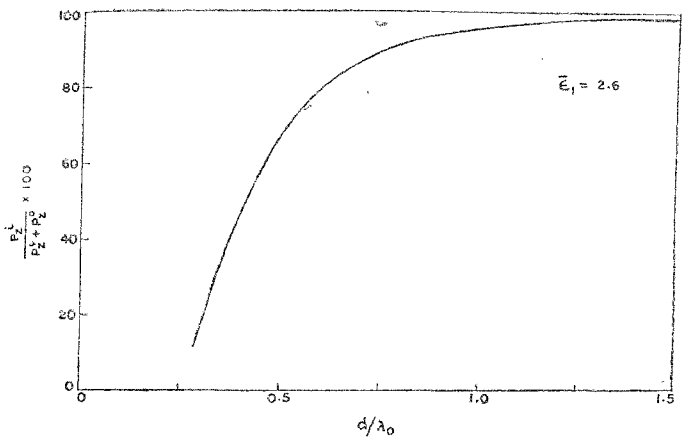


FIG. 10

Variation of power flow inside the rod as a percentage of the total power flow, with the diameter of the rod.
$P_z^1$=Power flow inside the therod. $P_z^0$=Power flow outside the rod

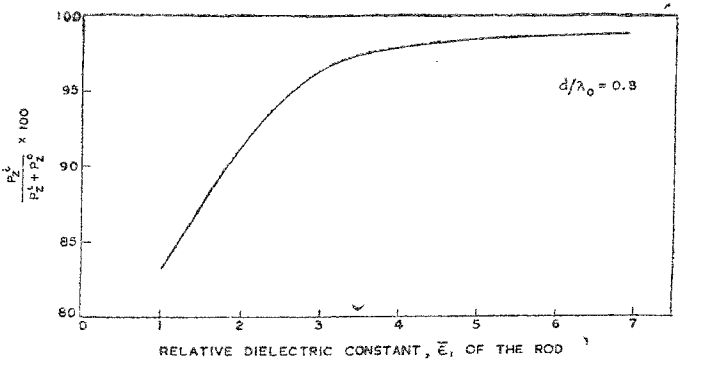


FIG. 11

Variation of power flow inside the rod as a percentage of the total power flow, with the relative dielectric constant of the rod.
$P_z^1$=Power flow inside the rod. $P_z^0$=Power flow outside the rod.

$P_{zn}$ represents the total power contained within a contour of radius $r_n$ and $r_1 < r_2 < r_3 \cdots < r_n$. The values of $P_{z1}$, $P_{z2}$, $\cdots$ $P_{zn}$ are determined from [21, 22] by replacing the integrals

$$\int_{\rho=a}^{\infty} \text{ by } \int_{\rho=a}^{\rho=r_1}, \int_{\rho=a}^{\rho=r_2}, \int_{\rho=a}^{\rho=r_3} \cdots \int_{\rho=a}^{\rho=r_n}$$

respectively. The constant percentage power contours and its respective radius for perspex rods ($\epsilon_1 = 2.6$) of different diameters excited in $HE_{11}$ mode have been evaluated (See figures 12 and 13)

## 9. Evaluation of the Field Components

By using appropriate field components of the $HE_{11}$ mode and applying proper boundary conditions, the following relation between the constants $B$, $b$, $c$ and $C$ are obtained.

$$\frac{C}{B} = \frac{x_1^2}{x_2^2} \frac{J_1(x_1)}{H_1^{(1)}(x_2)} = \delta \qquad [30]$$

$$\frac{c}{b} = \frac{x_1^2}{x_2^2} \frac{\epsilon_2}{\epsilon_1} \frac{J_1(x_1)}{H_1^{(1)}(x_2)} \qquad [31]$$

$$\frac{b}{B} = \frac{\gamma \epsilon_1}{i \omega \mu_0} \frac{x_1^2 - x_2^2}{x_1^2 x_2^2} \left[ \frac{x_1}{\epsilon_1} \frac{J_1'(x_1)}{J_1(x_1)} - \frac{\epsilon_2}{x_2} \frac{H_1^{(1)\prime}(x_2)}{H_1^{(1)}(x_2)} \right]^{-1} \qquad [32]$$

$$\frac{c}{C} = \frac{\gamma \epsilon_2}{i \omega \mu_0} \frac{x_1^2 - x_2^2}{x_1^2 x_2^2} \left[ \frac{\epsilon_1}{x_1} \frac{J_1'(x_1)}{J_1(x_1)} - \frac{\epsilon_2}{x_2} \frac{H_1^{(1)\prime}(x_2)}{H_1^{(1)}(x_2)} \right]^{-1} \qquad [33]$$

The constants $B$ and $C$ are expressed in terms of the total power flow $P_z$ along the guide as follows:

$$|B| = \left[ \frac{P_z}{X^2 + \delta^2 Y^2} \right]^{1/2} \qquad [34]$$

$$|C| = \delta \left[ \frac{P_z}{X^2 + \delta^2 Y^2} \right]^{1/2} \qquad [35]$$

since $$P_z = |B|^2 (X^2 + \delta^2 Y^2) \qquad [36]$$

Substituting $|B|$ and $|C|$ in [6 and 7], the field components of $HE_{11}$ mode inside and outside the guide are

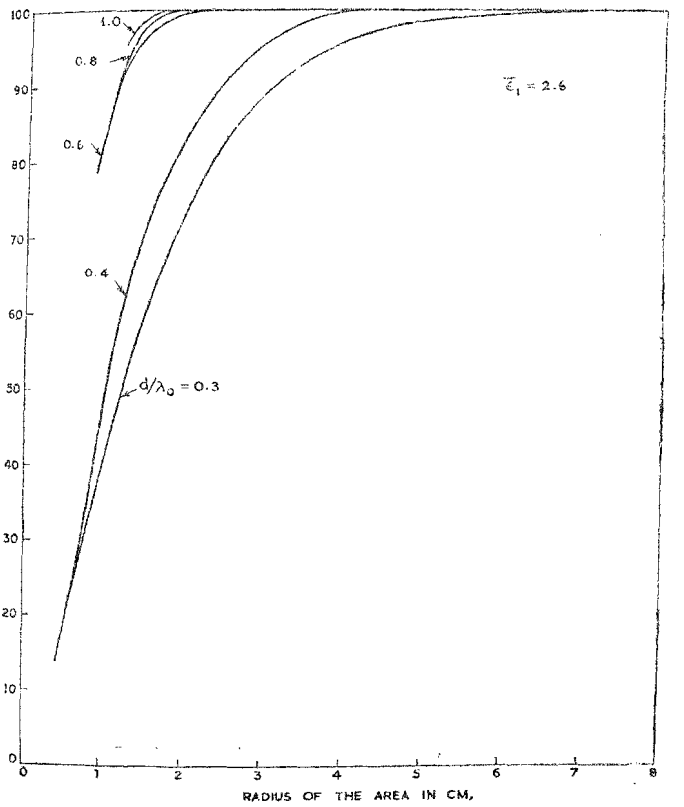


FIG. 12

Radius of the area around the dielectric rod vs. W%.
W% is the per cent of power surrounding the rod.

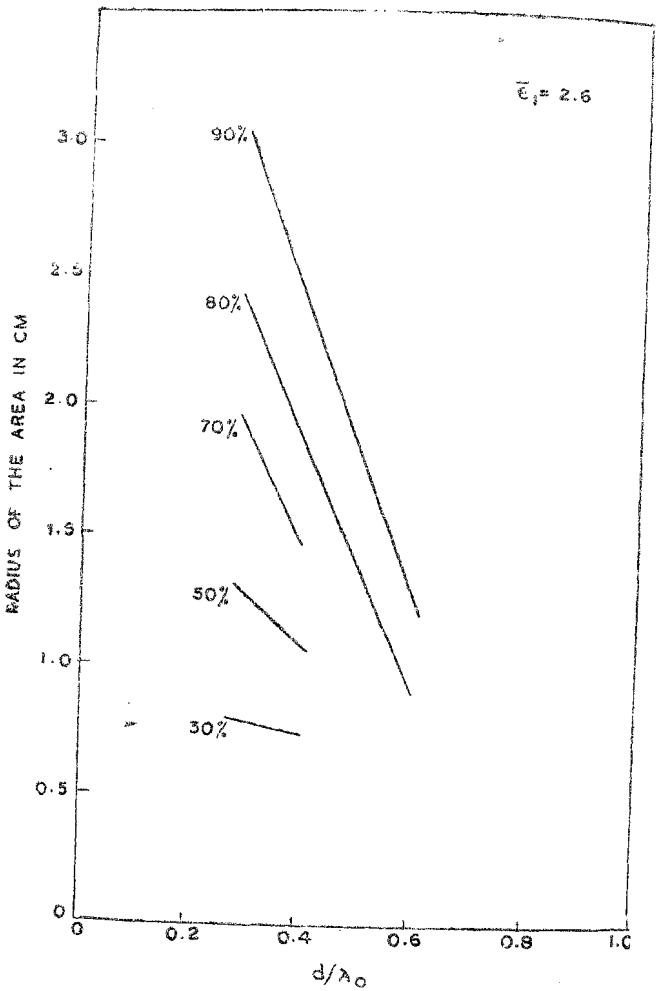


FIG. 13

Radius of the area around the dielectric rod within which 30%, 50%, 70%, 80 and 90% of the power is propagated as a function of the diameter of the rod.

Inside the guide (Region 1), $\rho \leqslant a$

$$E_{\rho 1} = -\left(\frac{P_z}{X^2 + \delta^2 Y^2}\right)^{1/2} \left(\frac{1}{\rho} J_1(k_1\rho) + \frac{b}{B} \frac{\gamma_1 k_1}{i\omega\epsilon_1} J_1'(k_1\rho)\right) \sin\phi \exp(-\gamma_1 z)$$

$$E_{\phi 1} = -\left(\frac{P_z}{X^2 + \delta^2 Y^2}\right)^{1/2} \left(k_1 J_1'(k_1\rho) + \frac{b}{B} \frac{1}{\rho} \frac{\gamma_1}{i\omega\epsilon_1} J_1(k_1\rho)\right) \cos\phi \exp(-\gamma_1 z)$$

$$E_{z1} = \left(\frac{P_z}{X^2 + \delta^2 Y^2}\right)^{1/2} \left(\frac{b}{B} \frac{k_1^2}{i\omega\epsilon_1} J_1(k_1\rho)\right) \sin\phi \exp(-\gamma_1 z) \qquad [37]$$

$$H_{\rho 1} = \left(\frac{P_z}{X^2 + \delta^2 Y^2}\right)^{1/2} \left(\frac{\gamma_1 k_1}{i\omega\mu_0} J_1'(k_1\rho) + \frac{b}{B} \frac{1}{\rho} J_1(k_1\rho)\right) \cos\phi \exp(-\gamma_1 z)$$

$$H_{\phi 1} = -\left(\frac{P_z}{X^2 + \delta^2 Y^2}\right)^{1/2} \left(\frac{1}{\rho} \frac{\gamma_1}{i\omega\mu_0} J_1(k_1\rho) + \frac{b}{B} k_1 J_1'(k_1\rho)\right) \sin\phi \exp(-\gamma_1 z)$$

$$H_{z1} = -\left(\frac{P_z}{X^2 + \delta^2 Y^2}\right)^{1/2} \left(\frac{k_1^2}{i\omega\mu_0} J_1(k_1\rho)\right) \cos\phi \exp(-\gamma_1 z)$$

Outside the guide, (Region 2), $\rho \geqslant a$

$$E_{\rho 2} = -\delta\left(\frac{P_z}{X^2 + \delta^2 Y^2}\right)^{1/2} \left(\frac{1}{\rho} H_1^{(1)}(k_2\rho) + \frac{c}{C} \frac{\gamma_2 k_2}{i\omega\epsilon_2} H_1^{(1)\prime}(k_2\rho)\right) \times \sin\phi \exp(-\gamma_2 z)$$

$$E_{\phi 2} = -\delta\left(\frac{P_z}{X^2 + \delta^2 Y^2}\right)^{1/2} \left(k_2 H_1^{(1)\prime}(k_2\rho) + \frac{c}{C} \frac{1}{\rho} \frac{\gamma_2}{i\omega\epsilon_2} H_1^{(1)}(k_2\rho)\right) \times \cos\phi \exp(-\gamma_2 z)$$

$$E_{z2} = \delta\left(\frac{P_z}{X^2 + \delta^2 Y^2}\right)^{1/2} \left(\frac{k_2^2}{i\omega\epsilon_2} H_1^{(1)}(k_2\rho)\right) \sin\phi \exp(-\gamma_2 z)$$

$$H_{\rho 2} = \delta\left(\frac{P_z}{X^2 + \delta^2 Y^2}\right)^{1/2} \left(\frac{\gamma_2 k_2}{i\omega\mu_0} H_1^{(1)\prime}(k_2\rho) + \frac{c}{C} \frac{1}{\rho} H_1^{(1)}(k_2\rho)\right) \times \cos\phi \exp(-\gamma_2 z)$$

$$H_{\phi 2} = -\delta\left(\frac{P_z}{X^2 + \delta^2 Y^2}\right)^{1/2} \left(\frac{1}{\rho} \frac{\gamma_2}{i\omega\mu_0} H_1^{(1)}(k_2\rho) + \frac{c}{C} k_2 H_1^{(1)\prime}(k_2\rho)\right) \times \sin\phi \exp(-\gamma_2 z)$$

$$H_{z2} = -\delta\left(\frac{P_z}{X^2 + \delta^2 Y^2}\right)^{1/2} \left(\frac{k_2^2}{i\omega\mu_0} H_1^{(1)} k_2\rho\right) \cos\phi \exp(-\gamma_2 z) \qquad [38]$$

The electric field components $E_\rho$, $E_\phi$ and $E_z$ are functions of $d/\lambda_0$ and $\epsilon_1$ (see figures 14, 15 and 16). The components $E_\rho$, $E_\phi$ and $E_z$ have been normalised with respect to their values at $\rho = a$. Since $E_\rho$ is discontinuous at $\rho = a$, it has been seperately normalised inside and outside with respect to the surface values $E'_\rho$ so that $E_\rho/E'_\rho$ vs $\rho$ curves (See fig. 14) are shown as continuous.

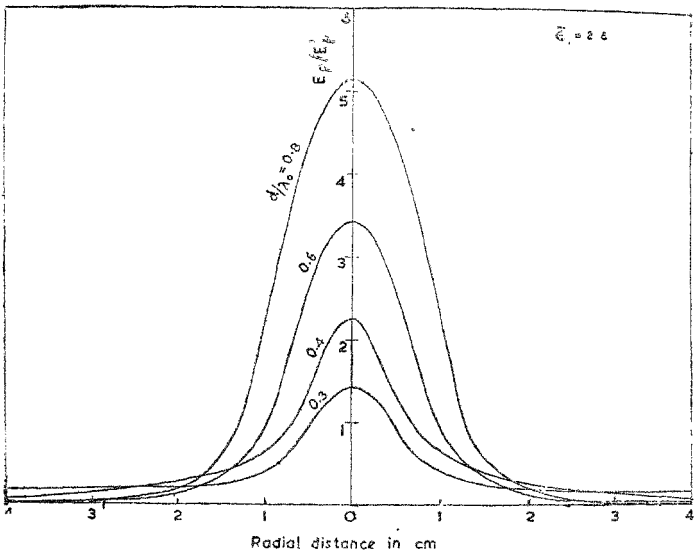


FIG. 14

Variation of the radial component $E_\rho$, of the electric field with the radial distance. $E'_\rho$ is the value of $E_\rho$ on the surface of the rod.

## 10. EXPERIMENTAL VERIFICATION OF FIELD DISTRIBUTION

Experimental determination (See figure 17) of the variation of $E_\rho$, $E_\phi$ and $E_z$ for the $HE_{11}$ mode in the radial direction shows fair agreement with the theory. The variation of only $E_\rho$ is represented graphically (see fig. 18). A monopole probe was used to measure $E_\phi$ and $E_\rho$ and a half wave dipole for $E_z$ components. The precision attenuator is adjusted for each value of $\rho$ to keep the output of the probe constant, so that the crystal in the tuner works

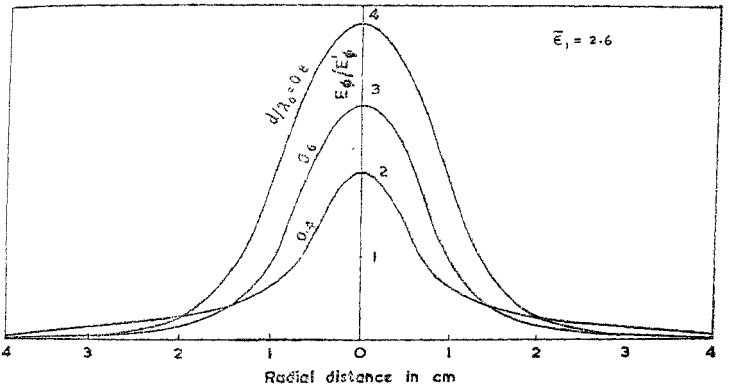


FIG. 15

Variation of the azimuthal component $E_\phi$, of the electric field with the radial distance. $E'_\phi$ is the value of $E_\phi$ on the surface of the rod.

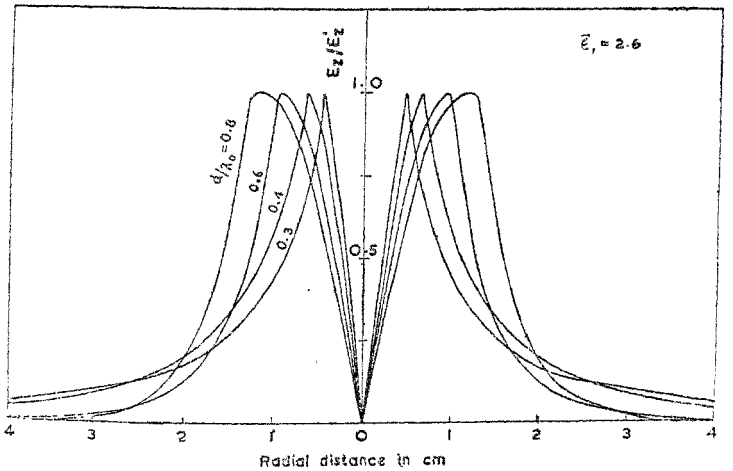


FIG. 16

Variation of the axial component $E_z$ of the electric field with the radial distance. $E'_z$ is the value of $E_z$ on the surface of the rod.

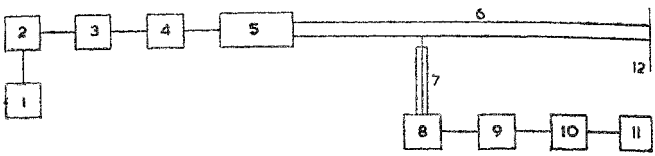


1. Regulated Power Supply with Square-Wave Modulator.
2. Klystron 723 A/B
3. Flap Attenuator
4. Frequency Meter PRD Type 586 A.
5. Mode Transformer with Collar.
6. Dielectric Rod Waveguide
7. Probe
8. Coaxial to Rectangular Adopter.
10. Broad Brand Crystal Mount-Prd Type 612/A
9. Precision Attenuator-Prd Type 185 B
11. Detector Amplifier.
12. Shorting Disc.

FIG. 17

Block schematic of experimental setup for the measurement of field components.

at constant input. This method eliminates the crystal law in field measurements. The experimental and theoretical values of $\lambda_g$ as a function of $d/\lambda_0$ for $HE_{11}$ mode and $\bar{\epsilon}_1 = 2.6$ derived from the standing wave pattern measurement along the guide show fair agreement (see fig 19). All measurements have been made at the X- band.

## 11. IMPEDANCE CHARACTERISTICS

The impedance characteristic of the dielectric guide is studied by considering it as a microwave network and determining the scattering matrix of the system consisting of the mode-transducer, and the dielectric rod. In order to determine the input impedance of the dielectric guide, it is necessary to transfer the impedance from the input to the output, of the mode transducer. The impedance parameters which are determined from the elements of the matrix enable the representation of the mode transducer as an equivalent T-network. The insertion loss and the transmission efficiency of the mode transducer are then determined. The launching efficiency of the transducer is then calculated from the elements of the scattering matrix.

### 11.1. CHARACTERISTICS OF THE MODE TRANSDUCER $H_{01}^{\square} - H_{11}^{\circ}$

By using Deschamp's[20] method (see figure 20), the scattering coefficients of the mode transducer were obtained and are as follows

$$S_{11} = 0.140 \text{ exp. } (i\ 203.7)$$
$$S_{12} = 0.969 \text{ exp. } (i\ 67.9) \qquad [39]$$
$$S_{22} = 0.143 \text{ exp. } (i\ 471.2)$$

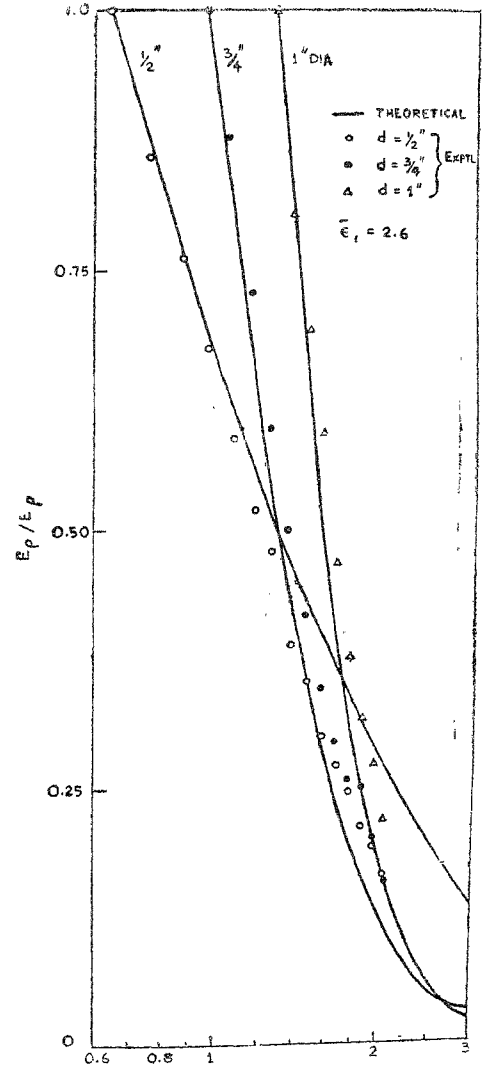
1.0
0.75
0.50
0.25
0
0.6
0.8
1
2
3
$E_p / E_p$
½"
¾"
1" DIA
THEORETICAL
d = ½"
d = ¾"
d = 1"
EXPTL
$\bar{\epsilon}_t = 2.6$

FIG 18

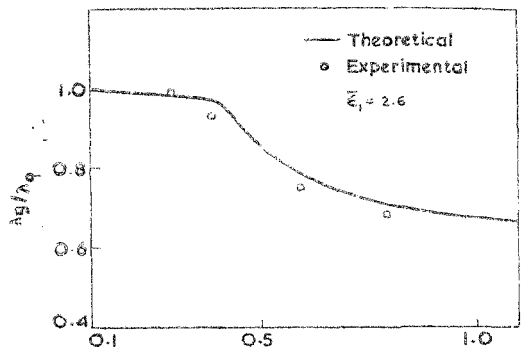


FIG. 19
Variation of the guide wavelength with the diameter of the rod.

The impedance parameters $Z_{11}$, $Z_{12}$ and $_{22}$ are obtained from the scattering coefficients by the following transformations.

$$Z_{11} = Z_1 \left( \frac{1 + S_{11} - S_{22} - [S]}{1 - S_{11} - S_{22} + [S]} \right) \qquad [40]$$

$$Z_{12} = \sqrt{(Z_1 Z_2)} \left( \frac{2 S_{12}}{1 - S_{11} - S_{22} + [S]} \right)$$

$$Z_{22} = Z_2 \left( \frac{1 - S_{11} + S_{22} - [S]}{1 - S_{11} - S_{22} + [S]} \right)$$

where, $[S] = S_{11} S_{22} - S^2_{12}$

$Z_1$ = Characteristic impedance of the mode transducer at the input terminals
= Characteristic impedance of the rectangular guide excited in $H_{01}$ mode
= 4.0 $\Omega$

$Z_2$ = Characteristic impedance of the mode transducer at the output terminals.
= Characteristic impedance of the circular metallic guide excited in $H_{11}$ mode.
= 436.5 $\Omega$

Substituting [39] in [40], the impedance parameters reduce to

$$Z_{11} = 9.385 + j\,119.2$$
$$Z_{12} = 2.994 + j\,427.7 \qquad [41]$$
$$Z_{22} = 9.645 + j\,204.6$$

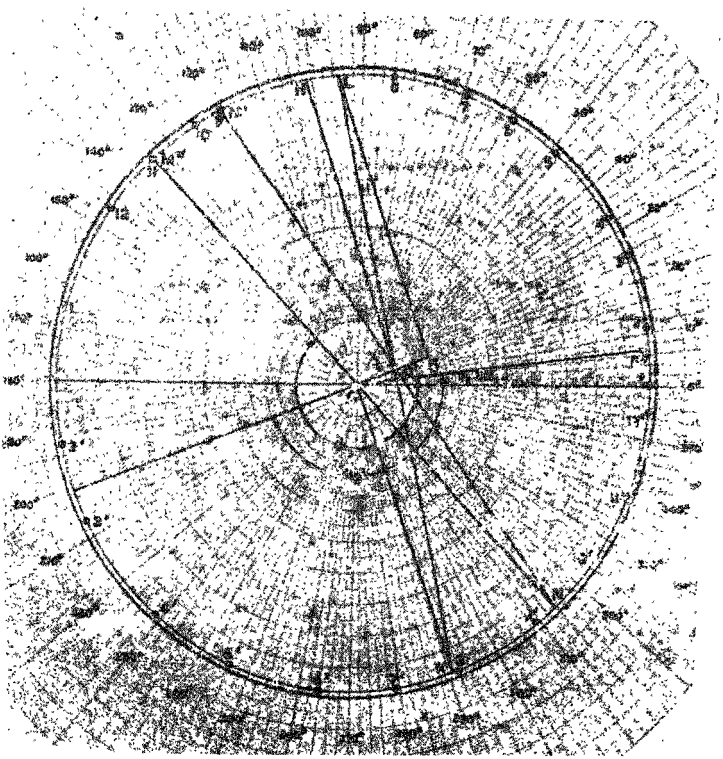

FIG. 20

Circle diagram showing theconstruction leading to the determination of the scattering coefficients of mode transducer

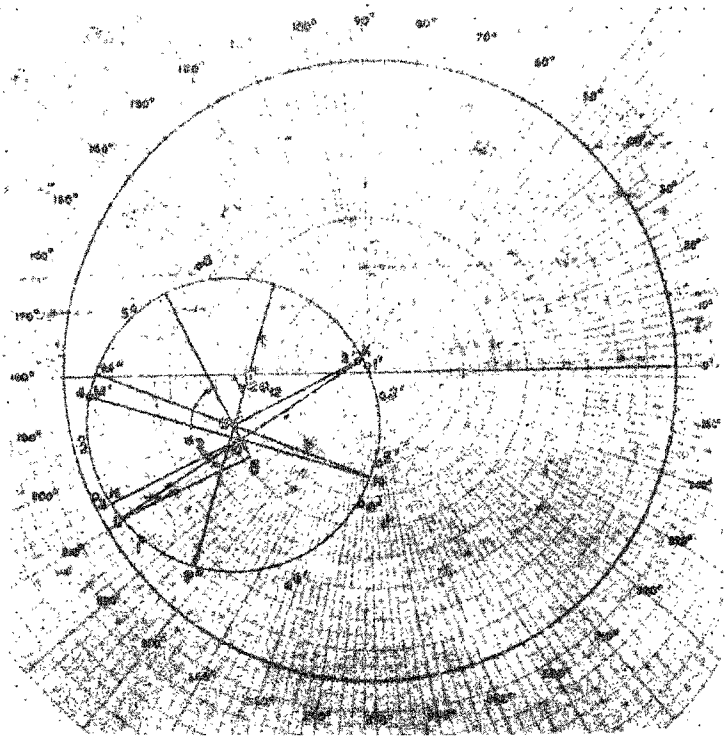

FIG 24

Circle diagram showing the construction leading to the determination of the scattering coefficients of the dielectric rod waveguide

which yields

$$Z_{11} - Z_{12} = 6.391 - j\,308.5$$
$$Z_{22} - Z_{12} = 6.651 - j\,223.1 \qquad [42]$$

The impedance parameters [41 and 42] lead to the representation of the equivalent T-network of the $H_{01}^{\square} - H_{11}^{0}$ mode transducer (see fig. 21)

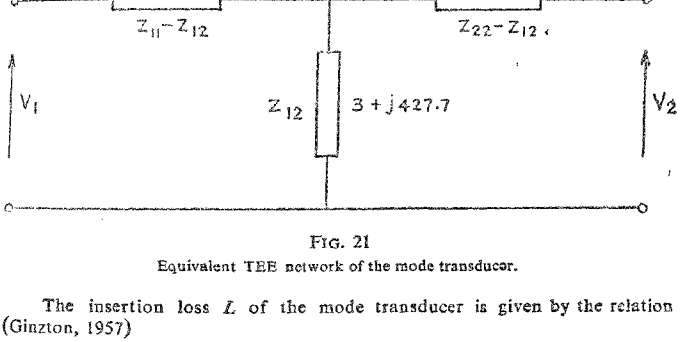


FIG. 21

Equivalent TEE network of the mode transducer.

The insertion loss $L$ of the mode transducer is given by the relation (Ginzton, 1957)

$$L(db) = -10\log_{10}(1-|S_{11}|^2) - 10\log_{10}|S_{12}|^2/(1-|S_{11}|^2) = 0.274\ db \qquad [43]$$

where, the reflection loss $L_R$ at the input terminals of the transducer is

$$L_R(db) = -10\log_{10}(1-|S_{11}|^2) = 0\ 086\ db \qquad [44]$$

and the dissipation loss in the network is

$$L_D(db) = -10\log_{10}|S_{12}|^2/1-|S_{11}|^2 = 0.188\ db \qquad [45]$$

The transmission efficiency $\eta_t$ of the mode transducer defined in terms of the scattering coefficients is

$$\eta_t = |S_{12}|^2/(1-|S_{11}|^2) = 95.76\% \qquad [45]$$

### 11.2 Input Impedance of the Dielectric Rod

By using the nodal shift method, the impedance as seen by the slotted section for different lengths of the dielectric rod is determined. The impedance seen by the slotted section is then transferred to the input end of the dielectric guide with the help of $A$, $B$, $C$, $D$ parameters which are as follows.

$$\begin{aligned} A &= (Z_{11}/Z_{21}) = \sqrt{(Z_1/Z_2)} \times 0.2754 \angle -4.1^\circ \\ B &= (|Z|/Z_{21}) = \sqrt{Z_1 Z_2} \times 0.9634 \angle -82.7^\circ \\ C &= (1/Z_{21}) = 1/\sqrt{(Z_1 Z_2)} \times 1.0360 \angle -89.6^\circ \\ D &= (Z_{22}/Z_{21}) = \sqrt{(Z_2/Z_1)} \times 0.4862 \angle -2.3^\circ \end{aligned} \qquad [47]$$

where, $$|Z| = Z_{11} Z_{22} - Z_{12}^2 \qquad [48]$$

The transformation of impedance from the input to the output end of the mode transducer is effected with the aid of the usual relation (see fig. 26*a*)

$$Z'' = (DZ' - B)/(CZ' - A) \qquad [49]$$

The input impedance of the dielectric rod guide as a function of the normalised length $l/\lambda_0$ has been evaluated (See fig. 22).

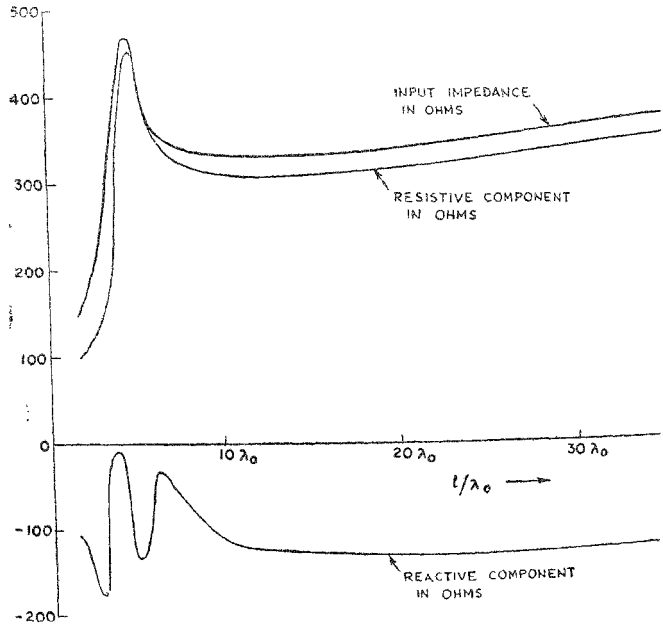


FIG. 22

Variation of input impedance with the length of the guide.

### 11.3 Characteristic Impedance

The conventional open circuit and short circuit method has been used to determine the open circuit impedance $Z'_{oc}$ when the dielectric rod is shorted at the free end and is of length $(l + \lambda_g / 4)$ from the feed end, and the short circuit impedance $Z'_{sc}$ when under the same condition, the length of the dielectric rod is changed to $l$ where, $l$ is an integral multiple of $\lambda_g$. The impedances $Z'_{oc}$ and $Z'_{sc}$ seen by the slotted section is then transferred to the input end of the dielectric rod. The characteristic impedance $Z_0$ of the dielectric guide is then evaluated as a function of the length of the dielectric rod (see fig. 23) in terms of the transformed impedances $Z_{oc}$ and $Z_{sc}$ from the relation.

$$Z_0 = \sqrt{(Z_{oc}\, Z_{sc})} \qquad [50]$$

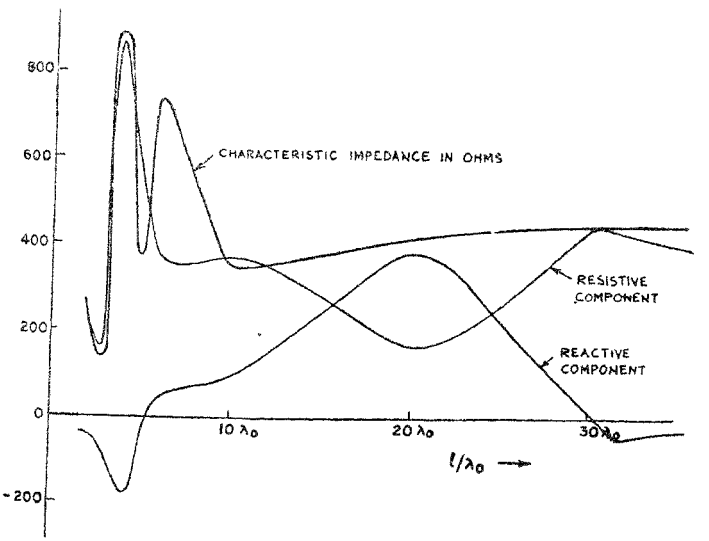


FIG. 23

**Variation of the characteristic impedance with the length of the guide.**

### 11.4 SCATTERING MATRIX OF THE DIELECTRIC GUIDE

The scattering matrix $\Sigma$ of the system composed of the mode transducer and the dielectric rod guide is determined by Deschamp's (1953) method. The complex reflection coefficients for different lengths of the dielectric guide is plotted (see fig. 24) as a circle diagram from which the scattering coefficients $\Sigma_{11}$, $\Sigma_{12}$ and $\Sigma_{22}$ are determined.

$$\Sigma_{11} = 0.048 \exp(j\,28)$$
$$\Sigma_{12} = 0.675 \exp(j\,35)$$
$$\Sigma_{22} = 0.093 \exp(j\,316) \qquad [51]$$

The scattering coefficients $\sigma_{11}$, $\sigma_{12}$ and $\sigma_{22}$ of the the dielectric rod guide is obtained in terms of the $S-$ matrix and $\Sigma-$ matrix (See Appendix A).

$$\Sigma_{11} = S_{11} + \left(\frac{S_{12}^2}{1 - \sigma_{11}\, S_{22}}\right) \sigma_{11}$$

$$\Sigma_{12} = S_{12}\left(\frac{\sigma_{12}}{1 - \sigma_{11}\, S_{22}}\right)$$

$$\Sigma_{22} = \sigma_{22} + \left(\frac{\sigma_{12}^2}{1 - \sigma_{11}\, S_{22}}\right) S_{22} \qquad [52]$$

which with [39 and 51] yield

$$\sigma_{11} = 0.1945 \exp(j\,69.1)$$
$$\sigma_{12} = 0.7161 \exp(-j\,32.9)$$
$$\sigma_{22} = 0.1191 \exp(-j\,81.8) \qquad [53]$$

### 11.5 LAUNCHING EFFICIENCY

The launching efficiency is expressed in terms of the $S$-matrix and $\sigma =$ matrix (see Appendix B)

$$\eta_L = \frac{1 - |\sigma_{11}|^2}{|1 - \sigma_{11}\, S_{22}|^2} |S_{12}|^2$$
$$= 85.5\% \qquad [54]$$

## 12. ATTENUATION CONSTANT

Assuming that there is no loss in the free space surrounding the dielectric rod, the power transmitted along the guide is

$$P_z = P_z^i + P_z^0$$

The power loss, $P_{dL}$ per unit length of the guide excited in $HE_{11}$ mode is

$$P_L = \frac{1}{2}\int_{\phi=0}^{2\pi}\int_{\rho=0}^{a} \sigma_1 |E|^2 \rho\, d\rho\, d\phi$$

$$= \frac{B^2}{2}\omega\epsilon_1 \tan\delta \left[ 2\pi\left(1 + \frac{b^2}{B^2}\frac{\beta_1^2}{\omega^2\epsilon_1^2}\right)\int_0^a \frac{1}{\rho}\{J_1(k_1\rho)\}^2 d\rho \right.$$

$$- 4\pi\frac{b}{B}\frac{\beta_1}{\omega\epsilon_1}\int_{\rho=0}^{a}\frac{1}{\rho}\{J_1(k_1\rho)\}^2 d\rho$$

$$+ \frac{b^2}{B^2}\frac{\pi k_1^4}{\omega^2\epsilon_1^2}\int_{\rho=0}^{a}\rho\{J_1(k_1\rho)\}^2 d\rho$$

$$+ \pi k_1^2\left(1 + \frac{b^2}{B^2}\frac{\beta_1^2}{\omega^2\epsilon_1^2}\right)\int_{\rho=0}^{a}\rho\{J_0(k_1\rho)\}^2 d\rho$$

$$- 2\pi k_1\left(1 + \frac{b^2}{B^2}\frac{\beta_1^2}{\omega^2\epsilon_1^2}\right)\int_{\rho=0}^{a} J_0(k_1\rho) J_1(k_1\rho)\, d\rho$$

$$\left. + 4\pi\frac{b}{B}\frac{\beta_1 k_1}{\omega\epsilon_1}\int_{\rho=0}^{a} J_0(k_1\rho) J_1(k_1\rho)\, d\rho \right] \qquad [55]$$

where, $\sigma_1 = \omega\epsilon_1 \tan\delta$

$\tan\delta$ = loss tangent of the dielectric rod = 0.005

and $|E|^2 = |E_{\rho 1}|^2 + |E_{\phi 1}|^2 + |E_{z1}|^2$

The attenuation constant

$$\alpha = P_L/2P_z \qquad [56]$$

has been evaluated and determined experimentally (see fig. 25) by using the v.s.w r. method and calculating $\alpha$ from the relation

$$\alpha = (1/l)\ \text{are tanh}\ (1/\text{v.s.w.r.}) \qquad [57]$$

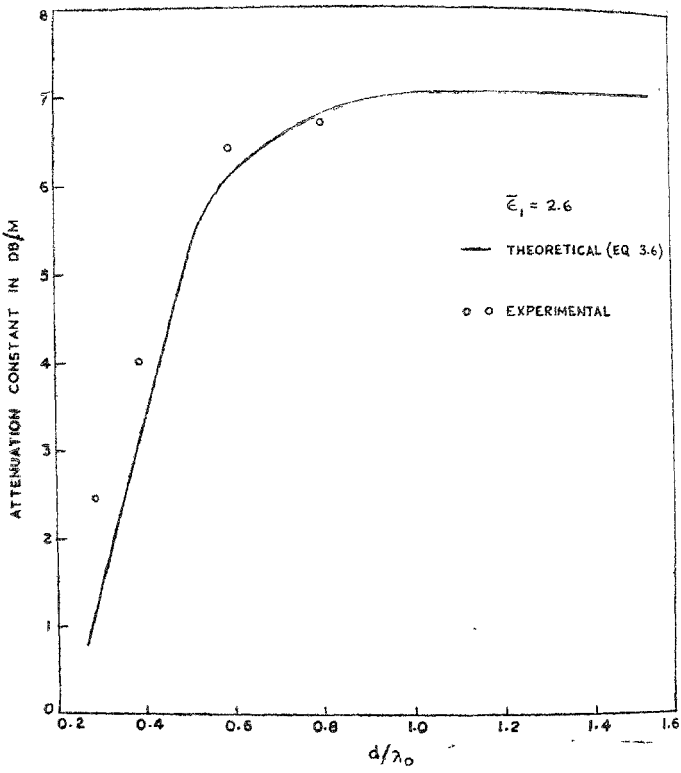


FIG. 35

Variation of attenuation constant of the dielectric rod waveguide with the diameter of the rod for the $HE_{11}$ mode.

## 13. Concluding Remarks

The investigations lead to the following conclusions

The radial propagation constant $k_2$ outside the rod increases with increasing $d/\lambda_0$ for all the three modes $E_{01}$, $E_{01}$ and $HE_{11}$ But $k_2\,(HE_{11}) > k_2\,(H_{01}) > k_2\,(E_{01})$ which means that in the radial direction outside the rod $(\text{Field spread})_{HE_{11}} < (\text{Field spread})_{H_{01}} < (\text{Field spread})_{E_{01}}$ as the argument of the Hankel function contains $k_2$.

The radial field spread outside the rod decreases with increasing values of $\bar{\epsilon}_{11}$ and $d$.

The axial phase constant increases at first with increasing $d/\lambda_0$ and tends in the limit to the value corresponding to that of a plane wave propagating in an infinite medium having $\mu$ and $\epsilon$ the same as that of the dielectric rod.

The symmetric modes $E_{01}$ and $H_{01}$ possess a cut-off wavelength depending on $d$ and $\bar{\epsilon}_1$ of the rod. But there is no such cut-off behaviour in the case of $HE_{11}$ mode. For small values of $d/\lambda_0$, $(\lambda_g/\lambda_0) \to 1$, which means that a major part of the power flows outside the guide.

As $d/\lambda_0$ increases, $\lambda_g/\lambda_0$ decreases and finally approaches asymptotically the value of $1/\sqrt{\bar{\epsilon}_1}$, which corresponds to the propagation of the wave through an infinite medium having a dielectric constant equal to $\bar{\epsilon}_1$.

The difference between the theoretical and observed variation of the electric field in the radial direction may be possibly due to the following causes. Higher order modes may be present due to the discontinuity present invariably at the junction between the mode transducer and the dielectric guide. Though the probes are placed in preferred direction for a particular component, other components may induce unwanted currents in the probe. The presence of the probe may also affect the measurement due to interaction between the probe and the guide.

The power flow in the radial and circumferential directions is reactive.

The division of power between the inside and outside of the guide for the three modes is compared as follows

$$\left(\frac{P_z^i}{P_z^0}\right)_{HE_{11}} > \left(\frac{P_z^i}{P_z^0}\right)_{H_{01}} > \left(\frac{P_z^i}{P_z^0}\right)_{E_{01}}$$

The oscillatory nature of the input impedance of the dielectric guide for lower values of $l/\lambda_0$ and its tendency to become fairly constant for higher values of $l/\lambda_0$ remain to be justified by theory.

## 14. APPENDIX – A

Scattering Matrix of the Dielectric Waveguide: Let $\begin{pmatrix} S_{11} & S_{12} \\ S_{21} & S_{22} \end{pmatrix}$ be the scattering matrix of the mode transducer and $\begin{pmatrix} \sigma_{11} & \sigma_{12} \\ \sigma_{21} & \sigma_{22} \end{pmatrix}$ be the scattering matrix of the dielectric rod guide only. Then, (See fig. 26)

$$\begin{pmatrix} E_{r1} \\ E_{r2} \end{pmatrix} = \begin{pmatrix} S_{11} & S_{12} \\ S_{21} & S_{22} \end{pmatrix} \begin{pmatrix} E_1 \\ E_2 \end{pmatrix} \qquad [A.1]$$

$$\begin{pmatrix} E_{r3} \\ E_{r4} \end{pmatrix} = \begin{pmatrix} \sigma_{11} & \sigma_{12} \\ \sigma_{21} & \sigma_{22} \end{pmatrix} \begin{pmatrix} E_3 \\ E_4 \end{pmatrix} \qquad [A.2]$$

So,

$$\begin{aligned} E_{r1} &= S_{11} E_1 + S_{12} E_2 \\ E_{r2} &= S_{21} E_1 + S_{22} E_2 \\ E_{r3} &= \sigma_{11} E_3 + \sigma_{12} E_4 \\ E_{r4} &= \sigma_{21} E_3 + \sigma_{22} E_4 \end{aligned} \qquad [A.3]$$

When the networks $S$ and $\sigma$ are connected, so that the terminals 2-2 and 3-3 are joined together

$$\begin{aligned} E_{r2} &= E_3 \\ E_2 &= E_{r3} \end{aligned} \qquad [A.4]$$

Substituting [A.4] in [A.2]

$$\begin{pmatrix} E_2 \\ E_{r4} \end{pmatrix} = \begin{pmatrix} \sigma_{11} & \sigma_{12} \\ \sigma_{21} & \sigma_{22} \end{pmatrix} \begin{pmatrix} E_{r2} \\ E_4 \end{pmatrix} \qquad [A.5]$$

which with [A.3] yields

$$E_2 = \frac{\sigma_{11} S_{12} E_1 + \sigma_{12} E_4}{1 - \sigma_{11} S_{22}} \qquad [A.6]$$

which with [A.3] yields

$$E_{r1} = \left[ S_{11} + \left( \frac{S_{12}^2}{1 - \sigma_{11} S_{22}} \right) \sigma_{11} \right] E_1 + S_{12} \left( \frac{\sigma_{12}}{1 - \sigma_{11} S_{22}} \right) E_4 \qquad [A.7]$$

Similarly,

$$E_{r2} = \frac{S_{12}\, E_1 + \sigma_{12}\, S_{22}\, E_4}{1 - \sigma_{11}\, S_{22}} \qquad [A.8]$$

$$E_{r4} = S_{12}\left(\frac{\sigma_{12}}{1 - \sigma_{11}\, S_{22}}\right) E_1 + \left[\sigma_{22} + \left(\frac{\sigma_{12}^2}{1 - \sigma_{11}\, S_{22}}\right) S_{22}\right] E_4 \qquad [A.9]$$

The composite matrix $\begin{pmatrix} \Sigma_{11} & \Sigma_{12} \\ \Sigma_{21} & \Sigma_{22} \end{pmatrix}$ of the mode transducer and the dielectric guide is given by the relation

$$\begin{pmatrix} E_{r1} \\ E_{r4} \end{pmatrix} = \begin{pmatrix} \Sigma_{11} & \Sigma_{12} \\ \Sigma_{21} & \Sigma_{22} \end{pmatrix} \begin{pmatrix} E_1 \\ E_4 \end{pmatrix} \qquad [A.10]$$

where the coefficients are

$$\Sigma_{11} = S_{11} + \left(\frac{S_{12}^2}{1 - \sigma_{11}\, S_{22}}\right) \sigma_{11} \qquad [A.11]$$

$$\Sigma_{12} = S_{12} \times \left(\frac{\sigma_{12}}{1 - \sigma_{11}\, S_{22}}\right) \qquad [A.12]$$

$$\Sigma_{22} = \sigma_{22} + \left(\frac{\sigma_{12}^2}{1 - \sigma_{11}\, S_{22}}\right) S_{22} \qquad [A.13]$$

which on substitution of the coefficients of $S$-matrix and $\Sigma$-matrix yield the coefficients of the $\sigma$-matrix.

## 15. Appendix – B

### Launching Efficiency

Assuming a matched load at the terminals 4 – 4 (see fig. 26) the launching efficiency $HE_{11}$ mode on the dielectric rod guide is derived as follows

$$E_4 = 0 \qquad [B.1]$$

From Appendix A

$$E_{r3} = \sigma_{11}\, E_3 \qquad [B.2]$$

$$E_{r4} = \sigma_{21}\, E_3 \qquad [B.3]$$

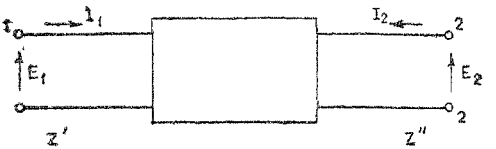


FIG. 26 (*a*)

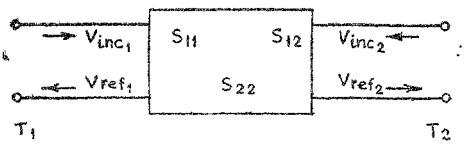


FIG. 26 (*b*)

Since S and $\sigma$ networks are cascaded

$$E_{r2} = E_3 \qquad \text{[B.4]}$$

$$E_2 = E_{r3} \qquad \text{[B.5]}$$

From Appendix A

$$E_2 = \sigma_{11}\, E_3 = \sigma_{11}\, E_{r2} \qquad \text{[B.6]}$$

$$E_{r2} = S_{21}\, E_1 + \sigma_{11}\, S_{22}\, E_{r2}$$

$$= \frac{S_{21}}{1 - \sigma_{11}\, S_{22}}\, E_1 \qquad \text{[B.7]}$$

Power entering the $\sigma$ – network

$$P_{\sigma 1} = |E_{r2}|^2 - (1 - |\sigma_{11}|^2)$$

$$= \frac{|S_{12}|^2}{|1 - \sigma_{11}\, S_{22}|^2}\,(1 - |\sigma_{11}|^2)\,|E_1|^2 \qquad \text{[B.8]}$$

Therefore, the launching efficiency is

$$\eta_L = \frac{P_{\sigma 1}}{P_{s1}} = \frac{(1 - |\sigma_{11}|^2)}{|1 - \sigma_{11}\, S_{22}|^2}\,|S_{12}|^2 \qquad \text{[B.9]}$$

where $P_{s1}$ represents the power incident on the S-network.

## References


1. Hondros, D. and Debye, P. .. .. *Annln. Phys* . 1910, **32**, 465.
2. Zahn, H. .. .. *Ann. Phys*., 1916, **49**. 907
3. Schriever, O. .. .. *Ibid*, 1920, **63**, 645.
4. Clarricoats, P. J. B. .. .. *Proc. Instn. elect. Engrs, P.T.C.*, 1961, **108**, 496.
5. Waldron, R. A. .. .. *J. Br. Instn. Radio Engrs*, 1958, **18**, 733.

5*a*. ———— , .. .. *Ibid*, 1958, **18**, 677.

6. Gillespie, E.F.F. .. .. *Proc Instn elec. Engrs, Pt. C.*, 1960, **107**, 198.
7. Clarricoats, P.J.B., and Waldron, R.A, .. *J. Electron. Control*, 1960, **8**, 455.
8. ———— , .. .. *Proc. Instn. elect. Engrs*, 1963, **110**, 261.
9. Brown, J. .. .. *J. Instn. Telecommun. Engrs* , 1963, **9**, 140.
10. Chandlor, C. H. .. .. *J. appl. Phys* , 1949, **20**, 1188.
11. Elsasser, W. M. .. .. *J. appl. Phys.*, 1949, **20**, 1193.
12. Du Hamel, R. H. and Duncan, J. W. .. *IRE Trans. microw, Theory Tech.*, 1958, **6**, 277.
13. Angulo, C. M. and Chang, W.S C. .. *Ibid*, 1958, **6**, 389.
14. ———— , .. .. *Ibid*, 1959, **7**, 207.
15. Duncan, J. W. and Du Hamel, R. H. .. *Ibid*, 1957, **5**, 284.
16. ———— , .. *Ibid*, 1959, **7**, 257.
17. Kay, A. F. .. .. *Ibid*, 1959, **7**, 22.
18. Brown, J. and Spector, J. O. .. *Proc. Instn. elect. Engrs., Pt. III* 1957, **104**, 27.
19. Weil, G. .. .. *Annls Radio elect.*, 1955, **10**, 228.
20. Deschamp, G. A. .. .. *Jour appl. Phys.* 1953, **24**, 1046.


## Additional Useful References


Wait, J. R. .. .. Electromagnetic Surface Waves, Advances in Radio Research, 1964, Vol. 4, Academic Press, 157-217.

Barlow, H. M., Brown, J. .. Radio Surface Waves, 1962. Clarendon Press,